International Journal Of Engineering Research And Development
e- ISSN: 2278-067X, p-ISSN: 2278-800X, www.ijerd.com
Volume 16, Issue 1 (Jan. 2020), PP.01-08

Infrared thermographic analysis of porous media simulated with spherical bodies

[1]Fikret Alic, [2]Alen Mešanović
[1]*Department of Thermal and Fluid Technique, Faculty of Mechanical Engineering, University of Tuzla*
[2]*Alen Mešanović, EPBiH, Tuzla Power, BOSNIA AND HERZEGOVINA*
Corresponding Author: Fikret Alic

ABSTRACT: *The spherical bodies are arranged in a multilayer manner within a cylindrical channel through which hot air flows with different volume flows. In this way, the spherical bodies form a porous fluid-heated medium, in this case air. The cylindrical hollow channel is thermally insulated so that the inlet heat of the fluid is converted to the heating of the spherical bodies and the heat output from the cylindrical channel. An infrared thermographic camera generates a thermogram of the porous medium of the outlet of a cylindrical channel, while directly measuring other process parameters. On the one hand, mathematical modeling determines the relationship between the effective temperature and the effective emissivity of a porous medium at different fluid flow rates and different emissivity of spherical bodies. The established methodology, mathematical modeling and infrared analysis give the possibility to determine the effective emissivity and the effective temperature of different porous structures.*

Date of Submission: 15-01-2020 Date of Acceptance: 31-01-2020

I. INTRODUCTION

The structure of the solid material in various practical applications can be porous and fluid or heat transfer possible through the same. A porous medium is a two-part material composed of cells (cavities or pores) and a solid material. Thus, the solid base cavities that are filled with a fluid, gas or liquid. Depending on the type and size of the porous cells, the velocity of the fluid flow and the properties and condition of the fluid, the thermal transfer between the fluid and the porous medium has different intensities. In addition to thermal transfer of various studies dealing with the pressure drop in the fluid passing through the porous medium. The material of the porous media is most commonly metallic or non-metallic, while the structure of the foam cells can be performed as an open cell or closed cell. Different types of porous media made from different base material, porosity and structure are used in different applications. M.F. Ashby (2000) and T.J.Lu (1998) studied the porosity can be extremely high, which directly reduces the mass of porous media. The technology of porous media production has evolved in several directions, depending on whether one wants to obtain a porous medium with open or closed cells.

Modern technological processes in the production of porous media with open cells enable different shapes and dimensions of cells. A. Bhattacharya et al.(2002), Xie,T et al.(2013), Liang, X.G and Wu.W (1999), and De Schampheleire, S et al.(2016) theoretical analyze and combined experimental tests of the effective conductivity of various metals and non-metallic porosity media were carried out by several authors. Connolly, M.P. (1992) showed the correlation between thermal diffusivity and medium porosity using pulsed infrared thermography. Hendorfer G. et al. (2006) quantitative tested porosity using active infrared thermography. F.Alic and A. Mešanović (2019) investigated the combined application of active infrared thermography when using non-metallic porous materials (ZrO_2) of different porosity.

In this paper, a porous medium was established using spherical particles, placed in a cylindrical channel through which heated air flows. The aim of the paper is to mathematically relate the forced convective excitation of a porous medium with the emitted thermal radiation.

Furthermore, the quantitative infrared analysis of thermograms determines the temperature field of the porous medium, that is, the effective emissivity and temperature of the porous medium on the outlet surface from the cylindrical channel.

II. MATERIAL AND METHODS

2. The analytical modeling of heat transfer through the porous layer

In the cylindrical channel of diameter D and height H are placed spherical bodies of diameter d_p, Figure 1. The heated fluid (air) temperature $t_{f.in}$ enters the bottom of the channel and convectively heats the spherical bodies. Fluid exits a cylindrical channel with some outlet temperature $t_{f.out}$. The cylindrical bodies, arranged in

multiple layers, form a simulated porous medium whose output surface has a mean emissivity of ε_{eff}. Because the cylindrical bodies are heated, they also emit thermal radiation at the outlet cross section of the cylindrical channel, which is thermally insulated from the environment, $q_{lost} = 0$.

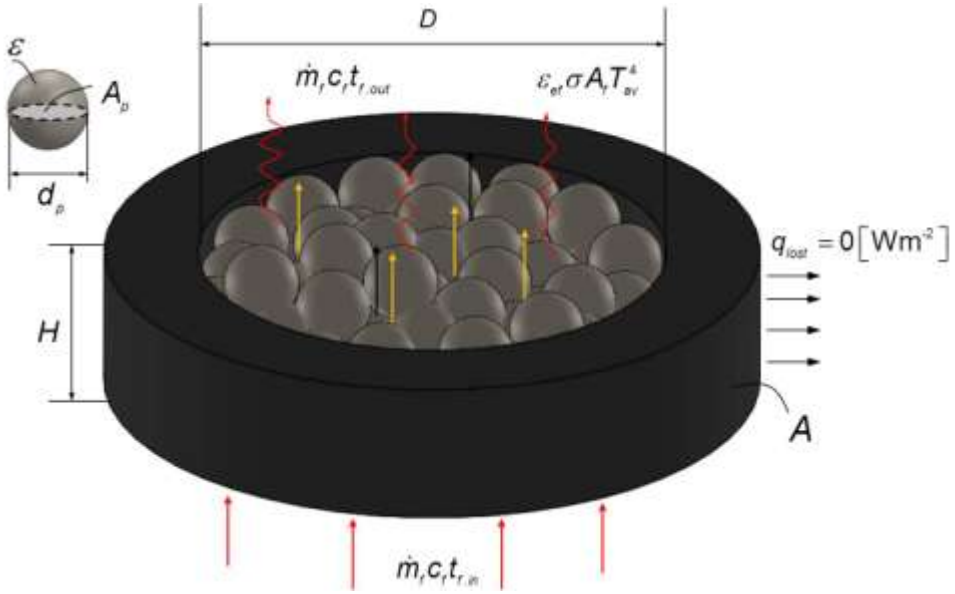

Figure 1: Thermal excitation of simulated porous media using spherical solids

According to Figure 1, thermal excitation of the spherical bodies with different emissivity is carried out, which makes it possible to establish an analytical modeling and obtain thermograms by infrared active thermography.

2.1. The porous medium consists of spherical bodies of the same emissivity

Since the cylindrical channel is thermally insulated, the total heat loss is considered negligible, so the heat balance takes the form

$$\dot{m}_f c_f T_{f.in} - \dot{m}_f c_f T_{f.out} = \sigma A \varepsilon_{eff} \bar{T}_{av}^4 \tag{1}$$

where $\dot{m}_f$ and c_f are mass flow and specific heat capacity of the fluid (air) respectively, while $T_{f.in}$ is inlet and $T_{f.out}$ outlet fluid from cylidrical channel.

The average temperature of the surface $\bar{T}_t$ and the effective emissivity ε_{eff} of the surface *A*. From equation (1), the average temperature of the output porous surface can be represented by the equation (2)

$$\bar{T}_{av} = \left[\frac{\dot{m}_f c_f \left(T_{f.in} - T_{f.out}\right)}{\varepsilon_{eff}\sigma A_f}\right]^{0.25} = \left[\frac{\rho_f w_f \left(T_{f.in} - T_{f.out}\right)}{\varepsilon_{eff}\sigma}\right]^{0.25} \tag{2}$$

where w_{fo} the velocity of the fluid is before entering the cylindrical channel. The velocity of the fluid w_f within the porous media is greater than the velocity w_{fo} due to the decrease in cross-section for fluid passage and depends on the porosity φ of the porous media through which the fluid flows. Heat balance within a porous medium located in a cylindrical channel is

$$\alpha A_{conv}\left(\bar{T}_f - \bar{T}_s\right) = \frac{1}{2}\alpha A_{conv}\left[\left(T_{f.in} + T_{f.out}\right) - \left(T_{s.in} + T_{s.out}\right)\right] = \dot{m}_f c_f \left(T_{f.in} - T_{f.out}\right) \tag{3}$$

from which the fluid outlet temperature of the porous matter is obtained, assuming that $T_{s.in} \approx T_{f.in}$,

$$T_{f.out} = \frac{2\dot{m}_f c_f T_{f.in} - \alpha A_{conv}\bar{T}_s}{2\dot{m}_f c_f + \alpha A_{conv}} \tag{4}$$

where *R* is the radius of the spherical bodies, *n* is the number of spherical bodies, *D* is the diameter of the channel within which the porous medium is located, and w_{fo} is the velocity of the fluid just before entering the porous medium, Figure 1. The convective coefficient α of the heat transfer from a fluid to a solid material of a porous medium, in the case of a laminar flow regime, can be determined using equation (5), [1],

$$\alpha = 0.664\,\mathrm{Pr}^{\frac{1}{3}}\,\mathrm{Re}_{\varphi}^{\frac{1}{2}}\,\frac{\lambda_f}{d_p} = 0.664\,\mathrm{Pr}^{\frac{1}{3}}\left(\frac{\mathrm{Re}}{\varphi}\right)_{\varphi}^{\frac{1}{2}}\frac{\lambda_f}{d_p} = 0.664\,\mathrm{Pr}^{\frac{1}{3}}\left(\frac{w_f d_p}{\nu_f \varphi}\right)_{\varphi}^{\frac{1}{2}}\frac{\lambda_f}{d_p} \tag{5}$$

where in the case of turbulent fluid flow is

$$\alpha = 0.59\,\frac{\lambda_f}{d_h}\,\frac{\varphi^{1.5}}{(1-\varphi)^{5/8}}\left(\frac{\mathrm{Re}-1}{\mathrm{Re}-1000}\right)^{0.25}\cdot \mathrm{Re}^{\frac{2}{3}}\,\mathrm{Pr}^{\frac{1}{3}} = \tag{6}$$

$$0.59\,\frac{\lambda_f}{d_h}\,\frac{\varphi^{1.5}}{(1-\varphi)^{5/8}}\left(\frac{\frac{w_f d_h}{\nu_f}-1}{\frac{w_f d_h}{\nu_f}-1000}\right)^{0.25}\cdot\left(\frac{w_f d_h}{\nu_f}\right)^{\frac{2}{3}}\mathrm{Pr}$$

where d_h is the hydraulic diameter of the particle i.e. body.

2.2. The porous medium consists of spherical bodies of the different emissivity

In case the spherical bodies are of different emissivity, while the other geometric characteristics remain the same, the thermal balance of thermal radiation on the output surface of the porous medium takes the form

$$\sigma A T_{eff}^4 \varepsilon_{eff} = n_1 \sigma A_1 \varepsilon_1 T_1^4 + n_2 \sigma A_2 \varepsilon_2 T_2^4 = n_1 \sigma A_1 \varepsilon_1 T_1^4 + n_2 \sigma \left(A - A_1\right) \varepsilon_2 T_2^4 \tag{7}$$

where n_1, and n_2 are the number of spheres of area A_1 and A_2, respectively. The emissions ε_1 and ε_2 refer to the individual surfaces A_1 and A_2, while A represents the total cross-sectional area of the cylindrical channel. The effective emissivity of the entire surface represented by the following equation,

$$\varepsilon_{eff} = \frac{n_1 A_1 \varepsilon_1 + n_2 \left(A - A_1\right)\varepsilon_2}{A} = \frac{n_1 d_{p1}^2 \varepsilon_1 + n_2 \left(D^2 - d_{p1}^2\right)\varepsilon_2}{D^2} \tag{8}$$

where d_{p1} and d_{p2} diameters of spherical bodies. The effective temperature of the outer surface of the porous medium is obtained by combining equations (7) and (8).

$$T_{eff} = \left[\frac{n_1 A_1 \varepsilon_1 T_1^4 + n_2 \left(A - A_1\right)\varepsilon_2 T_2^4}{n_1 A_1 \varepsilon_1 + n_2 \left(A - A_1\right)\varepsilon_2}\right]^{0.25} = T_1\left[\frac{1 + \frac{n_2}{n_1}\frac{\varepsilon_2}{\varepsilon_1}\left(\frac{D^2}{d_{p1}^2}-1\right)\left(\frac{T_2}{T_1}\right)^4}{1 + \frac{n_2}{n_1}\frac{\varepsilon_2}{\varepsilon_1}\left(\frac{D^2}{d_{p1}^2}-1\right)}\right]^{0.25} \tag{9}$$

Consider the case that spherical bodies of diameter d are placed concentrically within a cylindrical chennel of diameter *D*, as in Figure 2.

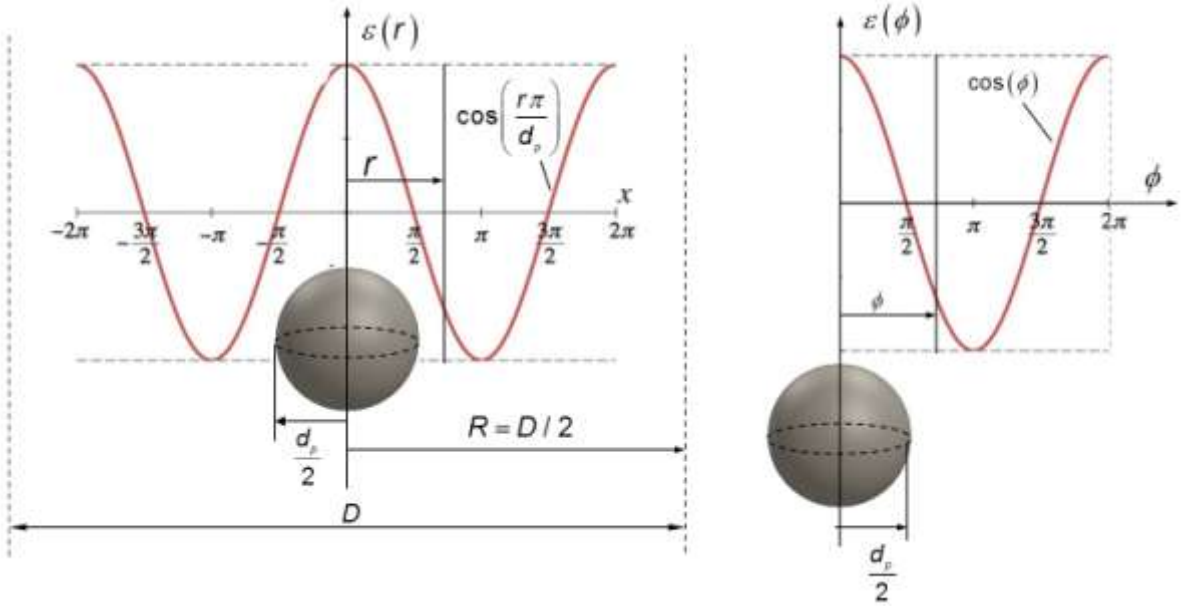

Figure 2: An example is the periodic distributions of the emissivity of spherical bodies by the radius and angle of cross-section of the channel

Let the emissivity of the surface vary by an approximate cosine function along the radius r and the angle ϕ, then the effective emissivity of that surface can be determined from

$$\varepsilon_{eff} = \frac{1}{2\pi}\int_0^{2\pi}\left(\frac{1}{R}\int_0^R \varepsilon(r,\phi)\,dr\right)d\phi = \tag{10}$$

$$\frac{1}{2\pi}\int_0^{2\pi}\left\{\frac{1}{R}\int_0^R \frac{1}{2}\left[(\varepsilon_1+\varepsilon_2)+(\varepsilon_1-\varepsilon_2)\cos\left(\frac{r\pi}{d_p}\right)\right]dr\right\}\cos\phi\,d\phi$$

where R is the radius of the cylindrical channel. In this case, the effective temperature of the output surface A of the porous medium is found using equation (11).

$$T_{eff} = \left\{\frac{n_1 A_1 \varepsilon_1 T_1^4 + n_2 (A - A_1)\varepsilon_2 T_2^4}{\frac{A}{2\pi}\int_0^{2\pi}\left\{\frac{1}{R}\int_0^R \frac{1}{2}\left[(\varepsilon_1+\varepsilon_2)+(\varepsilon_1-\varepsilon_2)\cos\left(\frac{r\pi}{d_p}\right)\right]dr\right\}\cos\phi\,d\phi}\right\}^{0.25} \tag{11}$$

III. RESULTS

The heated air of temperature $T_{f.in}$ and volumetric flow $\dot{V}_f$ enters a cylindrical channel, inside which is a porous medium. The porous medium represents a layer of non-metallic spheres, diameter d, arranged in several layers, Figure 1. The heated air flows between the spheres, thus heating them and leaving the cylindrical housing at a temperature of $T_{f.out}$. The cylindrical channel sheath is thermally insulated. Under stationary conditions, a thermogram of the surface of a porous medium with an infrared thermographic camera is taken from the front of the channel. Fluke Ti32 infrared was used in thermpgraphic imaging, while SmartView 2.32 thermogram analysis software was used. At the inlet to the cylindrical channel, the temperature and fluid flow were measured, while the ambient temperature was kept at 23°C. A control, measurement setup is presented in Figure 2, while the characteristic geometric characteristics of the channel and spherical bodies are shown within Table 2.

Table 1: Characteristic geometric dimensions of cylindrical channel and spherical bodies

D [m]	H [m]	d_1 [m]	d_2 [m]	n_1 [-]	n_2 [-]	ε_1 [-]	ε_2 [-]	c_f [$Jkg^{-1}K^{-1}$]	λ_f [$Wm^{-1}K^{-1}$]	ρ_f [kgm^{-3}]	Pr [-]
0.1	0.1	0.016	0.016	44	10	0.90	0.22	1016	0.035	0.815	0.701

3.1. Results and discussions

At a fluid inlet temperature of 168 ^oC, the fluid velocity within the porous medium was varied to 11ms^{-1}, while the fluid outlet temperature was indirectly determined and presented in Figure 2.

At maximum velocity within the porous medium of 11ms^{-1} was achieved at a volumetric flow rate of 0.005m^3s^{-1}. The outlet fluid temperature is highest at the minimum velocities to 1ms^{-1}, as the fluid for a long time retained in porous media.

Furthermore, the same figure shows a thermogram of the external output surface of a porous medium under given conditions, volumetric fluid flow of 0.005m^3s^{-1} and an inlet temperature of 168 ^oC.

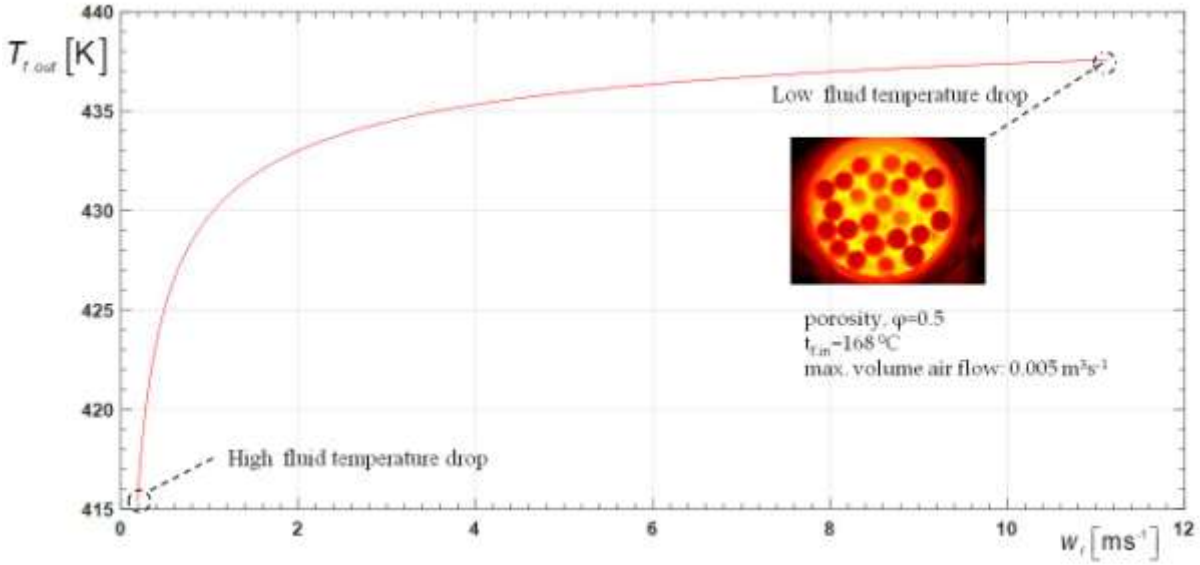

Figure 2: Air outlet temperature from porous medium, volumetric flow of 0.005 m^3s^{-1}

When the fluid velocity in the porous medium increases to 22ms^{-1}, the increase in fluid outlet temperature is approximately linear after 5ms^{-1}, Figure 3. To achieve a maximum fluid velocity within a porous medium of 22ms^{-1}, a volumetric fluid flow of 0.01m^3s^{-1} was used. In the case of an inlet fluid temperature of 164^oC and a volumetric flow rate of 0.01m^3s^{-1}, the outlet temperature value is shown in Figure 3.

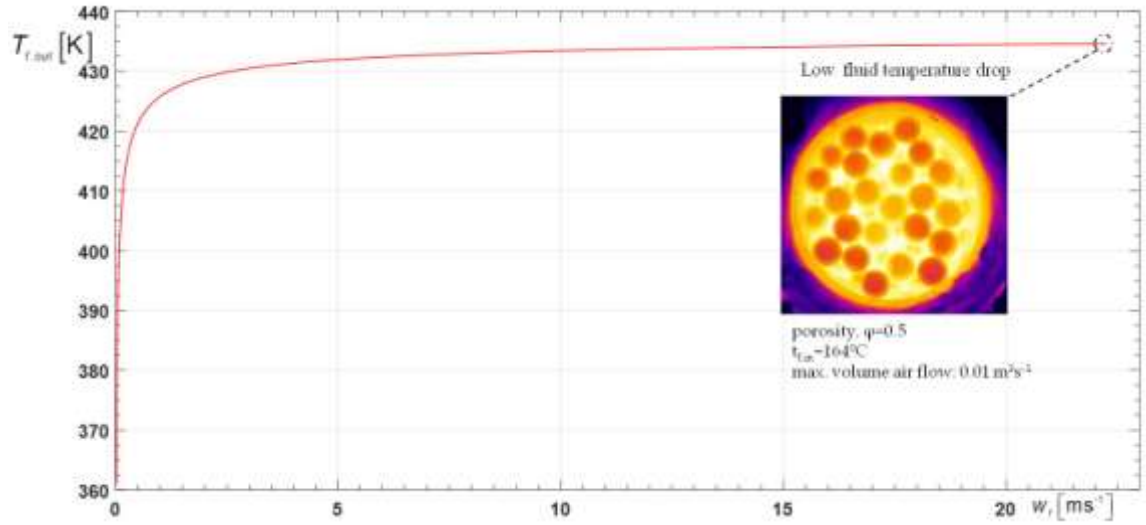

Figure 3: Air outlet temperature from porous medium, volumetric flow of 0.01 m^3s^{-1}

The same figure shows a thermogram of the output surface of a porous medium under given conditions, of 0.01m^3s^{-1} and an inlet temperature of 164 ^oC. The porosity of the medium was kept constant at 0.5, in both cases studied. Thermographic infrared analysis was performed using the Fluke Ti32 infrared thermographic camera, while thermogram processing was done using SmartView 2.32 software.

The temperature field of the porous medium obtained by spherical bodies is shown by a 3D thermogram, Figure 4.

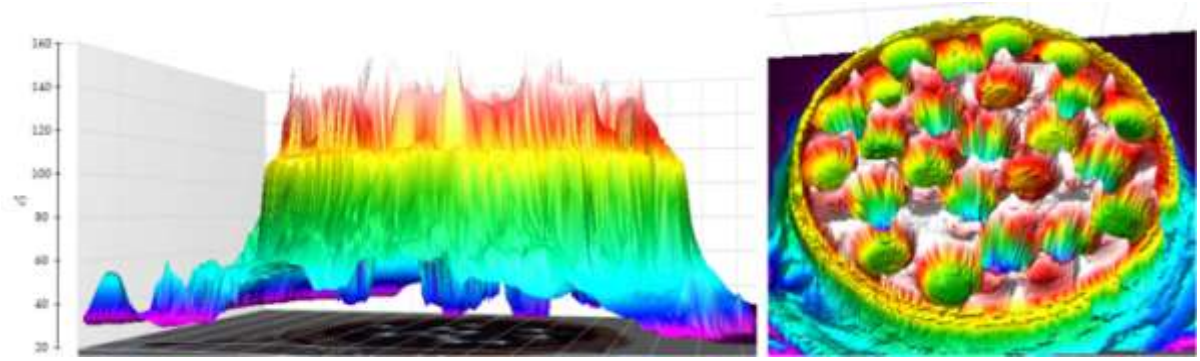

Figure 4: The temperature field of porous medium presented by 3D themogram

In the case of spheres of the same diameter and different emissivity, the thermogram of the output surface of the porous medium is shown in Figure 5. The marked areas in Figure 5 are known emissivity values of 0.22 and their total number is 10. Each marked surface (A0 ÷ A9) is associated with an average temperature (Avg). Also, for the whole cross section of the cylindrical channel, an average temperature of 121.66 ^oC was determined. The thermogram obtained in Figure 5a is valid for a fluid flow of 0.005 m^3s^{-1} and an inlet temperature of 165 ^oC. The same arrangement of spherical bodies of different emissivity within a cylindrical channel is subjected to a volumetric fluid flow of 0.01 m^3s^{-1} and an inlet temperature of 163 ^oC, Figure 5b.

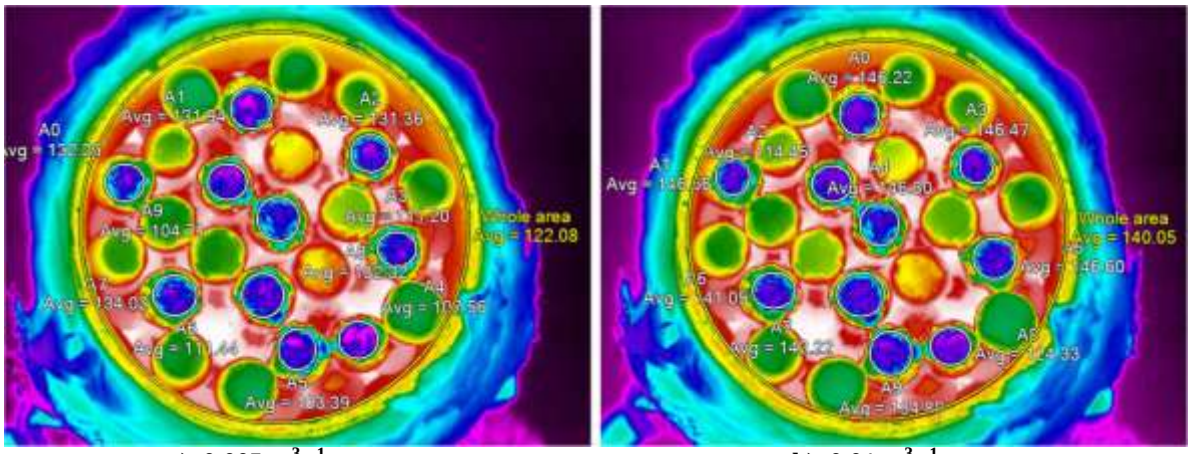

a) 0.005 m^3s^{-1} **b) 0.01 m^3s^{-1}**

Figure 5: Selective processing of thermograms of porous media with spherical bodies of different emissivity, at a flow of 0.005 m^3s^{-1} (Figure 5a) and 0.01 m^3s^{-1} (Figure 5b).

A specific analysis of the thermogram and interactions between bodies of the different emissivity and temperature is shown in Figure 6. Between two bodies of the same low emissivity and at about the same temperatures, the influence of reflected thermal radiation is negligible, region A. The spherical elements located deeper inside the cylindrical channel are at a higher temperature, region B. For this reason, region B is heated by thermal radiation and spherical bodies of higher emissivity, region C.

The correct geometric cross section is only noticeable in spherical bodies of higher emissivity ε_{high}, region D. On the spherical bodies of the low emissivity (ε_{low}), the enhanced influence of other spherical bodies of higher emissivity (ε_{high}) is clearly noticeable, region E, Figure 6.

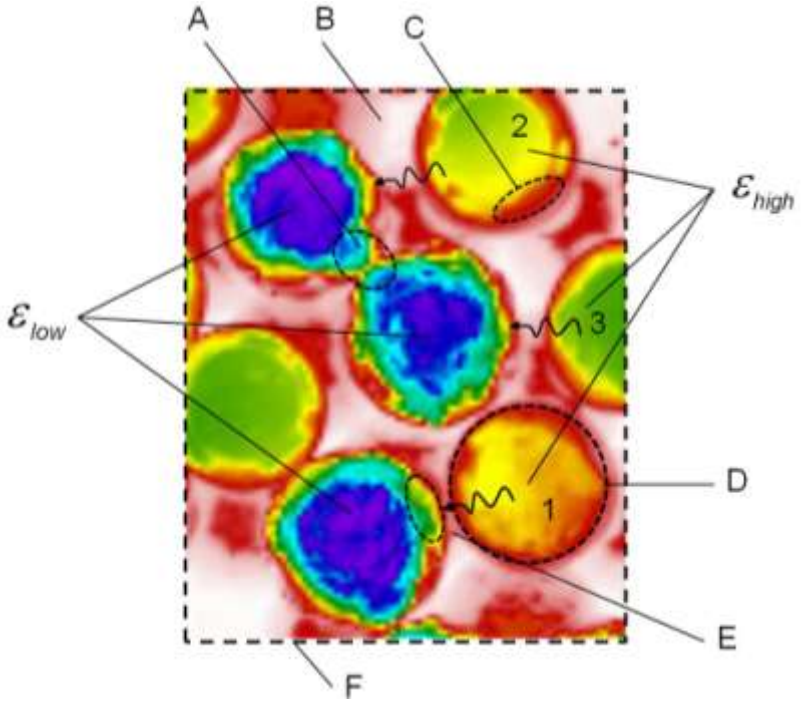

Figure 6: Characteristic thermogram regions of spherical bodies with different emissivity

If the body's emissivity is lower, the effect of the reflected radiation on the body is greater and the thermogram of the low emissivity body itself does not produce reliable results. On thermograms, region F, are denoted by 1,2,3, spherical bodies of higher emissivity, of ε_{high} = 0.9, while spherical bodies of low emissivity ε_{low} = 0.22.

In case the thermographic camera emissivity is set to 0.90, the spherical bodies of low real emissivity of 0.22 will show much lower apparent temperatures, areas A, B, and C, Figure 7.

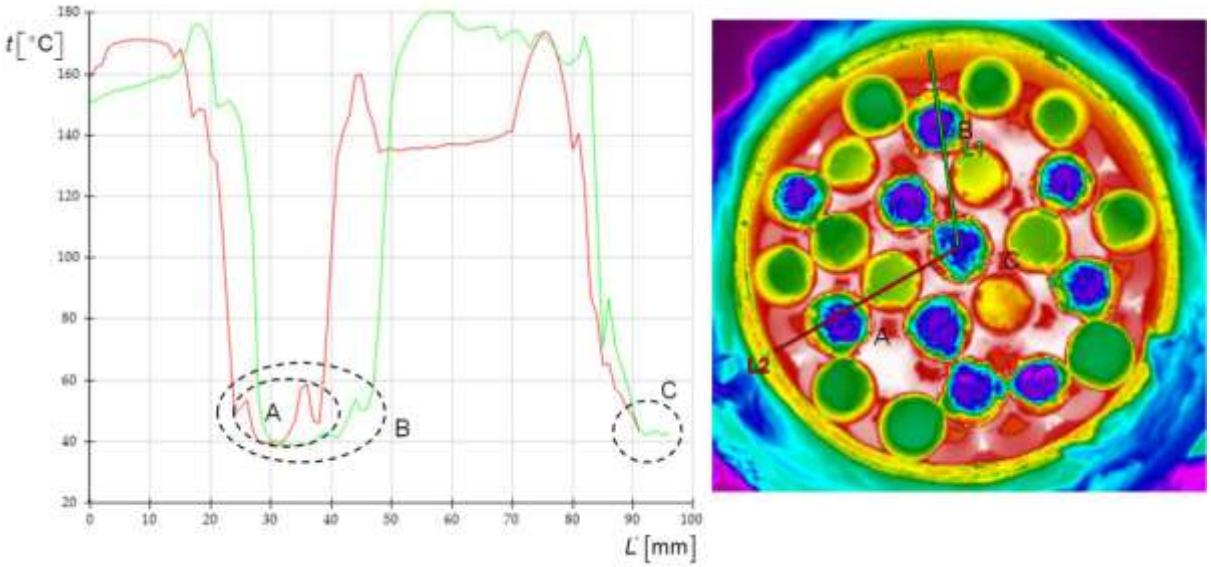

Figure 7: The apparent temperature profile of the surface of the porous medium, when the emissivity is not adjusted and amounts to 0.90 for all spherical bodies, at a volumetric flow of 0.01 m^3s^{-1}.

IV. DISCUSSION AND CONCLUSION

The solid spherical bodies are placed inside a cylindrical channel through which the heated air flows at different velocities. The cylindrical hollow channel is thermally insulated so that the inlet heat is converted to the heating of the spherical bodies and the output heat. The output heat consists of the output fluid enthalpy and the thermal radiation energy of the porous solid surface. A combination of mathematical modeling and

experimental testing yielded fluid outlet temperatures from a system designed in this way. With constant porosity, the outlet temperature of the fluid is a function of its inlet temperature and volumetric flow rate.
The emitted thermal radiation of the outer porous surface is a function of its temperature, emissivity, and the total radiating surface. Infrared thermographic analysis obtained thermograms of the output porous surface. According to the obtained thermograms, the mean temperatures of the outer porous surface were determined. Mean temperatures were analyzed in the case of the same and different emissivity of spherical bodies within a cylindrical channel. Spherical surfaces of different emissivity were located and mathematical expressions for the effective emissivity of a porous surface were established. The established methodology, mathematical modeling and infrared analysis, gives the possibility to determine the effective emissivity and effective temperature of different porous structures.

REFERENCES

[1]. Ashby, M. F.,(2000). Metal foams : a design guide. Boston ; Oxford: Butterworth-Heinemann.
[2]. Lu,T.J., Stone, H. A., and M. Ashby, F.,(1998). Heat transfer in open-cell metal foams. Acta Materialia, 46, 3619-3635.
[3]. Bhattacharya, A., V., Calmidi, V., and Mahajan, R. L.,(2002). Thermophysical properties of high porosity metal foams. International Journal of Heat and Mass Transfer,45, 1017-1031.
[4]. Xie, T., He, Y.L., Hu, Z.J.,(2013). Theoretical study on thermal conductivities of silica aerogel composite insulating material. Int. J. Heat Mass Transf., 58, 540–552.
[5]. Liang, X.G., Qu, W.,(1999). Effective thermal conductivity of gas-solid composite materials and the temperature difference effect at high temperature. Int. J. Heat Mass Transf., 42, 1885–1893.
[6]. De Schampheleire, S., De Jaeger, P., De Kerpel, K., Ameel, B., Huisseune, H., De Paepe, M.,(2016). How to study thermal applications of open-cell metal foam: Experiments and computational fluid dynamics. Materials , 9, 94.
[7]. Connolly, M. P.,(1992). The Measurement of Porosity in Composite Materials using Infrared Thermography. Journal of Reinforced Plastic Composites, 2,1367-1375.
[8]. Hendorfer G., Mayr G., Zauner G., Haslhofer M. and Pree R.,(2006). Quantitative Determination of Porosity by Active Thermography. 26th Review of Progress in Quantitative Non-Destructive Evaluation Proceeding, Portland (USA), Thompson D.O., Chimenti D.E. ed., 702-708.
[9]. Alic, F.,and Mešanović, A.,(2019). Active infrared thermography analysis of porous media PPI 10 and PPI 30 of ZrO_2. American Journal of Engineering Research, 8, 168-174.

1Fikret Alic "Infrared thermographic analysis of porous media simulated with spherical bodies" International Journal Of Engineering Research And Development, vol. 16 (1), 2020, pp 01-08.